Image Anal Stereol 2024;43:211-219 doi: 105566/ias.3289
*Original Research Paper*

# REFERENCE AREAS SELECTION AFFECTS REGISTRATION OF AI-SEGMENTED MANDIBLES ACQUIRED WITH CBCT

KLEMEN LEOPOLD[1], ALEŠ FIDLER✉[,2,3], MANUSHAQE SELMANI BUKLETA[4], MILAN KUHAR[1,5]

[1]University of Ljubljana, Faculty of Medicine, Department of Prosthodontics, Vrazov trg 2, 1000 Ljubljana, Slovenia; [2]University of Ljubljana, Faculty of Medicine, Department of Endodontics and Operative Dentistry, Vrazov trg 2, 1000 Ljubljana, Slovenia; [3]University Medical Centre Ljubljana, Department of Restorative Dentistry and Endodontics, Hrvatski trg 6, 1000 Ljubljana, Slovenia; [4]Alma Mater Europaea Campus Kolegji Rezonanca, Prosthodontic, Glloku te Shelgjet "Vetrnik", 1000 Prishtine, Kosova; [5]University Medical Centre Ljubljana, Department of Prosthodontics, Hrvatski trg 6, 1000 Ljubljana, Slovenia.

e-mail: klemen.leopold@mf.uni-lj.si; ales.fidler@mf.uni-lj.si; manushaqeart@gmail.com; milan.kuhar@mf.uni-lj.si

*(Received July 17, 2024; revised September 9, 2024; accepted October 9, 2024)*

ABSTRACT

Precise registration of sequential 3D datasets is crucial for accurate dimensional analysis. Utilizing the Local Best-Fit (LBF) algorithm and stable Registration Reference Areas (RRAs) facilitates the accurate alignment of 3D surface models. Currently, Cone-beam Computed Tomography (CBCT) and Deep Learning (DL) algorithms are at the forefront for segmenting CBCT scans to monitor morphological changes in the residual alveolar ridge. This study compares the effectiveness of different RRAs in registration sequential 3D surface models of partially edentulous mandibles. DL-assisted software segmented two sequential CBCTs (T0 and T1) from 10 patients, producing sequential 3D mandibular models. These models were aligned using three distinct RRAs: (i) WHOLE, encompassing the entire surface model; (ii) MND_BODY, covering the mandibular body while excluding the unstable alveolar ridge; and (iii) SPIN_FOR, incorporating stable RRAs (mental foramina and mental spine). An innovative method assessed registration accuracy by generating centroids from cross-sectional outlines of the mandibular nerve canals at the anterior third (A), medial third (B), and posterior third (C) of the posterior edentulous areas. The distance between centroids at T0 and T1 quantified registration accuracy. The MND_BODY group exhibited superior accuracy, whereas the SPIN_FOR group showed the least, with accuracy decreasing from A to C, suggesting rotational misalignments. When selecting RRAs, both stability and spatial distribution must be taken into account. For optimal alignment, sequential 3D surface models should use RRAs that are both stable and widely distributed.

Keywords: Computer assisted image processing, Cone-beam Computed Tomography, Deep learning, Dental models, Partial Denture, Three-dimensional imaging.

## INTRODUCTION

Precise registration of medical images is an increasingly important topic as it is a prerequisite for accurate detection of small differences between 3D structures. Numerous methods for the registration of 3D surface models of the jaw have been described in the recent literature, including landmark-based, surface-based (Stucki and Gkantidis 2020a), voxel-based approaches (Häner *et al.* 2020) and enhanced versions of these methods (Song 2015). Previous studies have provided evidence that the registration of surface models requires selection of Registration Reference Areas (RRAs) to achieve accurate Local Best-fit (LBF) alignment (O'Toole *et al.* 2019; Kuralt and Fidler 2021; Revilla-León *et al.* 2022). Kuralt *et al.* proposed a surface-based method that employed stable RRAs of the mandible for registration of sequential partially edentulous CBCT models (Kuralt *et al.* 2019; Kuralt *et al.* 2022). Recently, artificial intelligence (AI)-supported software, specifically DL, has shown promising results and is becoming state-of-the-art for segmentation of the mandible, including the mandibular nerve canal (Verhelst *et al.* 2021; Cui *et al.* 2022; Lahoud *et al.* 2022; Oliveira-Santos *et al.* 2023; Tan *et al.* 2024).

Residual ridge resorption occurring after tooth loss, a progressive lifelong process influenced by multiple factors throughout a person's life, (Tallgren 1972) has become increasingly important as it affects the future treatment planning with implants and prosthodontic appliances (Spencer 2018). In the past, studies have investigated the evaluation of residual ridge resorption using

various techniques such as sequential cast models or standardized radiographic methods like lateral cephalography or panoramic radiography (Kondo *et al.* 2023). More recently, CBCT has been frequently utilized for assessing morphological changes in the jaws (Ahmad *et al.* 2013). However, we still lack quality clinical studies of the field, and such data can be obtained by precise 3D evaluation.

This study aimed to compare registration accuracy with different RRAs for models, acquired with AI-segmentation of CBCT images. The null hypothesis was that there would be no significant difference in the data distribution among three registration methods across all cross-section positions.

# MATERIALS AND METHODS

## Study design and data acquisition

The present research paper represents a registration optimization for analysis of partially edentulous mandibles. Since registration step is crucial in the process of sequential 3D models evaluation, there was a need to evaluate registration methods and its accuracy. Ethical approval was obtained from the Ethics Committee of the Hospital and University Clinical Service of Kosovo and the University Clinical Centre of Kosovo (555/18.05.2017). All patients were informed of the study protocol and gave their written consent to participate. All patients were non-growing adults, both males and females aged between 45 and 65 years. They were classified as partially edentulous with bilaterally shortened dental arch (class I of the Kennedy classification system) and were provided with removable partial dentures. The inclusion criteria stated that patients had no previous prosthodontic treatment and were without active caries lesions or periodontal disease.

This study of two sequential CBCT scans taken from patients (n=10) who underwent clinical and radiological examination at the beginning of the study (T0) and at the follow-up, after one year (T1). All CBCT scans were performed using the same device (ORTHOPHOS XG 3D – Dentsply Sirona) with the following settings: field of view (FOV) of 8 x 8 cm, voxel size of 0.16 $mm^3$, 85 kV, and 7 mA for female patients and 10 mA for male patients. The data were exported in DICOM format.

## Segmentation

The DICOM files were uploaded to a cloud-based platform (Virtual Patient Creator, RELU BV, Leuven, Belgium) for AI-assisted segmentation. This platform offers automated segmentation of the entire maxillofacial complex, including teeth (Shaheen *et al.* 2021), jaws (Verhelst *et al.* 2021; Preda *et al.* 2022a), and the mandibular nerve canal with the mental foramen (Lahoud *et al.* 2022). The segmented mandibular models were exported as surface meshes in STL format for further analysis. Based on the time of capture, the models were labelled as T0 or T1.

## Registration

The STL data of the surface models were imported into GOM Inspect software (version 2018, GOM GmbH). Initially, the T0 models were registered by setting the matrix to align the body of the mandible with the z-axis of the global coordinate system. That orientation of the mandible facilitated further analysis. Separate registrations were performed for the left and right sides of the mandible.

Next, RRAs, like those described in the study by Kuralt *et al.* were created (Kuralt *et al.* 2019). Mental spines, which were clearly visible on the segmented surface models, were marked using surface curves. Mental foramina boundaries were defined using “To max. curvature” setting, which created spherical outlines. An offset curve around this sphere was constructed, which then served as a consistently selected RRA.

For the T1 models, a rough registration was performed with the T0 models using the "Prealignment" function. For final alignment, the LBF, which functions similarly to the Iterative Closest Point (ICP) algorithm (Besl and McKay 1992), was utilized using three different RRAs as presented on Fig. 1. (i) WHOLE, the entire surface model, excluding teeth; (ii) MND BODY, where mandibular body only (excluding unstable alveolar bone); (iii) SPINFOR method was carried out, using mental foramina and mental spine.

For each registration method, the T0 model was designated as the target element, and the T1 model was moved based on the transformation matrix generated by the software. Each registration outcome was labelled and saved for further analysis.

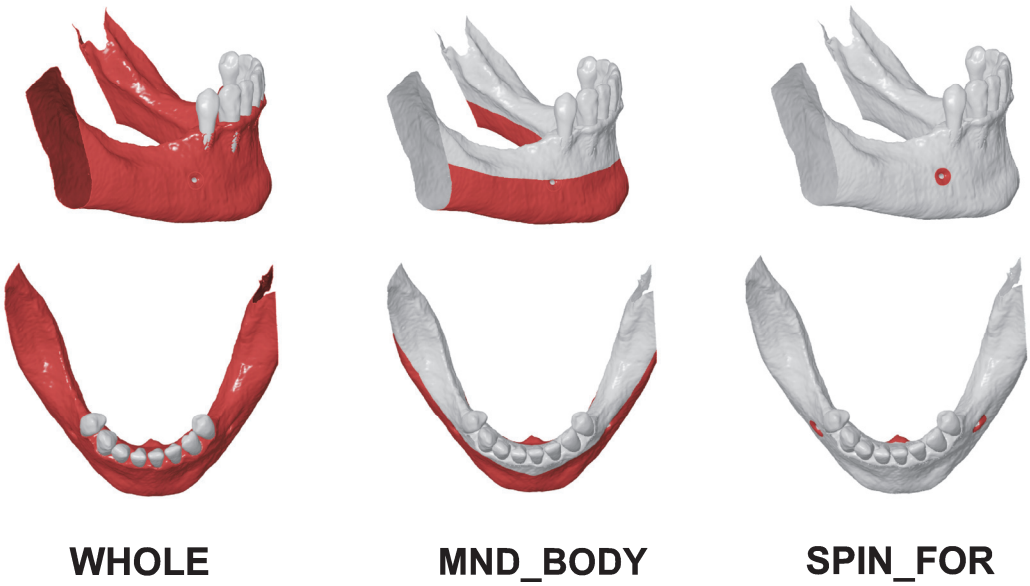


Fig. 1. *Registration reference areas - RRAs (marked with red), used for local best fit registration, represented on the same mandibular 3D model in the lateral (upper) and occlusal (lower) view. WHOLE - entire mandible without teeth; MND_BODY - including mandibular body, and SPIN_FOR - mental foramina and mental spine.*

## Evaluation

Before the registration, three cross-sections were constructed on both sides of the posterior edentulous ridge: A (anterior third), B (middle third), and C (posterior third). The cross-sections were generated in the bucco-lingual direction of the edentulous alveolar ridge, specifically the x-y plane of the global coordinate system. This resulted in 2-dimensional outlines of the mandible and the mandibular nerve canal. A centroid (geometric centres) corresponding to each outline of the mandibular nerve canal was created by the software as shown on Fig. 2. For each surface model (T0 and T1), three different centroids were obtained from each side of the mandible (A, B, and C test site for the left and right sides).

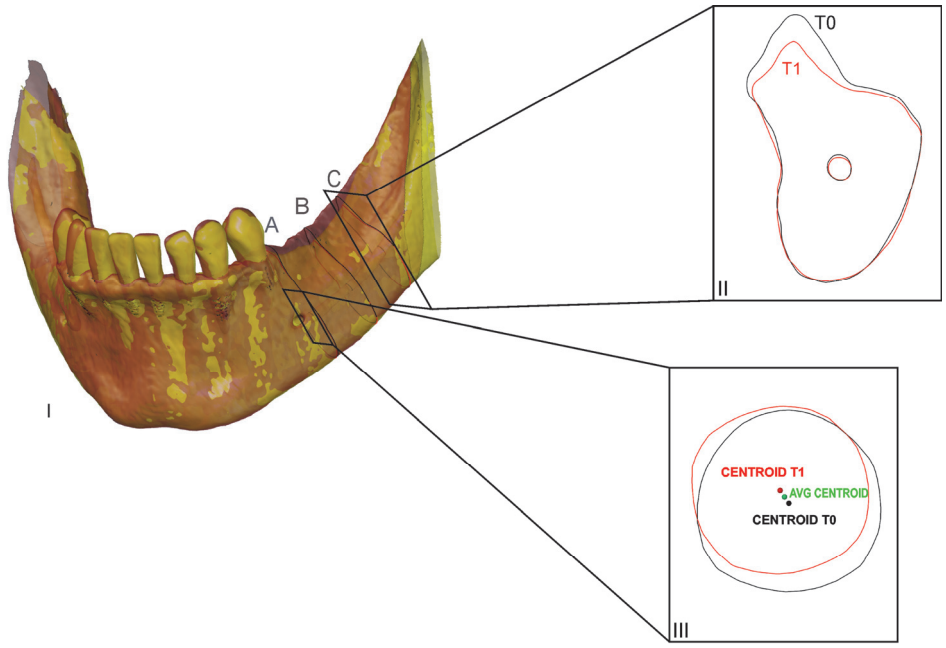


Fig. 2: *Evaluation of superimposition accuracy. I – mandible model, showing position of cross-sections A, B and C in posterior edentulous part. II – cross-sections of model T0 (black outline) and model T1 (red outline), III – outline of T0 (black outline) and T1 (red outline) in mandibular canal cross-sections along with their corresponding centroids (dots). The green point represents the average (AVG) centroid position of T0 and T1.*

Since the centroids obtained from the outlines of the mandibular canals were incorporated as reference points, mitigation of the potential impact of segmentation inaccuracies of the mandibular canals on the subsequent evaluation was needed. An additional registration of all the models (T1 to T0) was performed. The selected RRAs consisted exclusively of the left and right mandibular nerve canals for LBF alignment, referred to as MND.

The geometric data of centroids were imported into Microsoft Excel (Microsoft Corporation, 2018, Microsoft Excel). From previously exported MND alignment data, midpoints (AVG) between the centroids were calculated to minimize potential mandibular nerve canal segmentation errors. Then, Euclidean distances between Cartesian coordinates of AVG and centroid positions generated by other three registration methods being evaluated (SPIN_FOR, MND_BODY and WHOLE) were calculated. A greater distance between the centroids of a particular alignment method and the AVG centroids indicates a greater misalignment with respect to that method and the specific location of the cross section in question. Calculated distances were grouped according to the cross-section locations (A, B, and C) and registration methods (SPIN_FOR, MND_BODY and WHOLE).

### Statistical analysis

The statistical analysis was performed using SPSS software (IBM Corp., released 2020, IBM SPSS Statistics for Windows, Version 27.0, Armonk, NY: IBM Corp). The normality of the data distribution was assessed using the Kolmogorov-Smirnov and Shapiro-Wilk tests.

To compare the deviations from the reference centroids (AVG) between registrations with different RRAs at the same section locations (A, B, C), the Kruskal-Wallis test was utilized. Subsequently, post-hoc pairwise comparisons were performed using the Bonferroni correction method to account for multiple comparisons with a p-value of less than 0.05.

## RESULTS

The results of the Kolmogorov-Smirnov and Shapiro-Wilk tests indicated that the data distribution was non-normal. Consequently, non-parametric statistical tests were used for the analysis.

The Kruskal Wallis tests revealed that there was a significant difference between the data distribution of three superimposition methods for all cross-section locations ($p<0.002$; $p<0.000$; $p<0.000$; for section A, B and C, respectively). Post-hoc test revealed that SPIN_FOR group differed significantly from groups WHOLE and MND_BODY. Groups MND_BODY and WHOLE did not differ significantly.

The descriptive statistics showed a higher data dispersion in the SPIN_FOR group, with dispersion increasing from cross-section A to C. In the SPIN_FOR group, median deviation was 0.38 mm (IQR=0.24 mm, 0.54 mm), 0.40 mm (IQR=0.21 mm, 0.74 mm) and 0.53 mm (IQR=0.28 mm, 0.97 mm), for the cross-section A, B and C, respectively. As represented in the Fig. 3, the median deviation of the WHOLE and MND_BODY groups, were smaller and did not increase from cross-section A to C.

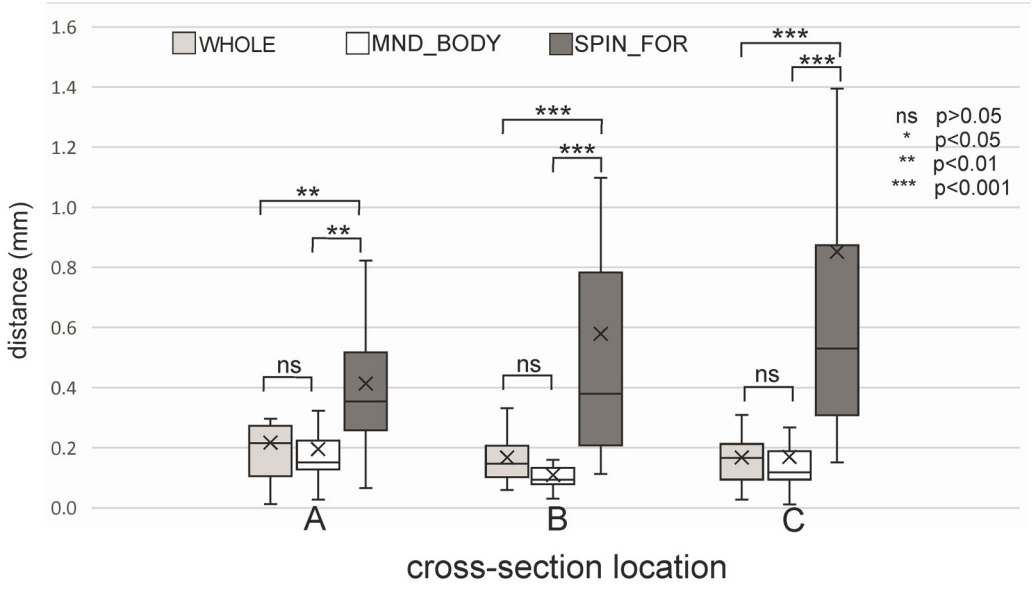


Fig. 3: *Deviations of three alignment groups (WHOLE, MND_BODY and SPIN_FOR) at three sites (A, B and C).*

The analysis of the raw data of the Cartesian coordinates of the centroids reveals that most of the deviations occur either in the coronal (maximum deviation = 1.61 mm) or in the apical direction (maximum deviation = 3.11 mm). The deviations in the buccal and lingual directions are significantly smaller (maximum deviation = 0.28 mm and 0.68 mm respectively). The average deviation in the apico-coronal direction was 0.34 mm at the site A cross-section, 0.53 mm at site B and 0.82 mm at site C. The average deviations in the bucco-lingual direction were 0.18 mm, 0.18 mm and 0.17 mm at sites A, B and C, respectively.

## DISCUSSION

Results of our study indicate that selection of RRA affects registration accuracy for state-of-the-art AI-segmented mandibles, with MND BODY being most accurate. Selection of RRA should consider not only stability but also spatial distribution.

Among three RRAs evaluated in our study, the highest accuracy was achieved by MND_BODY, closely followed by WHOLE, while SPIN_FOR exhibited significantly higher inaccuracy. The deviation of SPIN_FOR was found to be increasing from mesial to distal direction (from cross-section A to C), while for WHOLE and MND BODY the discrepancy was smaller and similar for all three test sites. This can be explained by spatial distribution of the RRAs. In SPIN_FOR, the RRAs were positioned near each other in the anterior part of the mandible. An imaginary axis, passing in the left-right direction allowed a rotation misalignment, which was increasing with distance from the axis, i.e., from mesial to distal direction. In contrast, MND_BODY and WHOLE, the RRAs covered a wider area, facilitating more precise registration in all regions. Similar results can be observed by some previous studies (Stucki and Gkantidis 2020b; Kuralt and Fidler 2021). It is worth noting that the boxplots depicted in Fig. 3 are derived from the Euclidean distances between centroids, which do not provide information about the translation direction of the mandibular 3D model. Raw data examination, considering the mismatch direction, revealed that the rotation misalignment in the apico-coronal was several-fold higher than the bucco-lingual direction, which further confirms the imaginary axis theory.

A best-fit alignment method, employing ICP algorithm, represents a robust method for precise registration of 3D surface models (Li *et al.* 2020). Previous studies from various fields of dentistry have shown that employing an LBF alignment method, where selected RRAs exclude dimensionally unstable parts, leads to increased

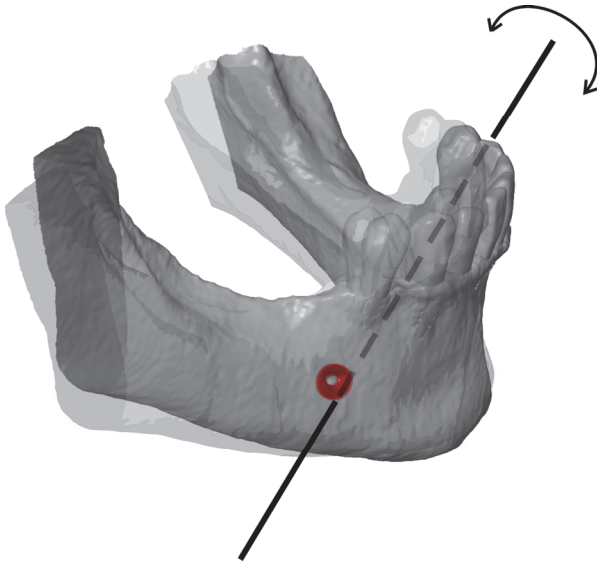

Fig. 4. *An imaginary axis around which the mandible 3D model is rotated when using SPIN_FOR RRA.*

registration accuracy. In contrary, whole-model best-fitt ing, including unstable areas in the RRA, resulted in less accurate registration (O'Toole *et al.* 2019; Kuralt and Fidler 2021; Revilla-León *et al.* 2022). One would expect similar findings when registering volumetrically unstable sequential 3D jaw models with changes from alveolar bone resorption. In this regard, study of Kuralt *et al.*, used only stable RRAs for LBF alignment, namely spinae mentalis and mental foramens, recognizing the potential pitfalls of including areas prone to volumetric instability due to bone resorption (Kuralt *et al.* 2019). However, above-stated approach didn't fully account for the importance of the spatial distribution of the RRAs. Results of the present study indicate that spatial distribution of the RRAs could play a crucial role in registration accuracy. The performance of the WHOLE group is somewhat counterintuitive, as it performed similarly well to the MND_BODY group, although it includes the alveolar ridge, which is prone to resorption. This can be attributed to the relatively short follow-up period and the resulting low resorption rates, which limits the scope of the present study. Working with more resorbed T1 mandibular models may have led to greater inaccuracies in registration when WHOLE RRA was employed. In the rapidly evolving field of digital dentistry, it's imperative to constantly reassess past research and maintain a critical perspective on our own methodologies. This underscores the necessity for ongoing critical evaluation and refinement of methodologies in the dynamic landscape of digital dentistry. Within the literature, various RRAs have been proposed for 3D jaw models registration, most commonly for orthodontic patients where jaw growth is still present (De Oliveira Ruellas *et al.* 2016; Nguyen *et al.* 2018; Stucki and Gkantidis 2020b). While

it is widely accepted that RRAs should represent stable anatomical landmarks, an optimal spatial distribution of these landmarks, particularly for the mandible, has not been determined.

Digital technologies such as AI, are widespread in dental image analysis (Schneider *et al.* 2022). Its high effectiveness and efficiency show great promise in dentistry (Rischke *et al.* 2022). Current state-of-the-art segmentation process for CBCT data therefore heavily relies on AI-assisted software (Wang *et al.* 2021). In addition to time efficiency, AI-assisted segmentation software represents improvement in limiting confirmation bias of the research papers, which can be present in manual segmentation and reduce operator variability (Schwendicke and Krois 2022). Nevertheless, it is important to note that AI models are constantly improving and therefore should be subjected to thorough evaluation and scrutiny (Schwendicke *et al.* 2020; Ma *et al.* 2022). The segmentation software utilized in our study has undergone extensive validation and has demonstrated promising results (Shaheen *et al.* 2021; Verhelst *et al.* 2021; Lahoud *et al.* 2022), with high standard research reports (Schwendicke *et al.* 2021). It uses the CNN approach, which is the most commonly used DL algorithm in image analysis. Specifically, a two-layer 3D U-network architecture was developed, which consists of two training steps. It was trained on 80 high-resolution CBCT datasets in DICOM format. They reported excellent accuracy and consistency of the metric parameters in comparison with standard semi-automatic segmentation. The reported mean Intersection over unit (IoU) parameter was above 94% and the mean Dice coefficient score (DSC) value was above 97% (Verhelst *et al.* 2021). Despite the beforementioned promising outcomes, the limited availability of the training data for AI models emphasizes the necessity for expert supervision - intelligent analysis (IA) of the AI (Liu *et al.* 2019; Mohammad-Rahimi *et al.* 2023). In conjunction with visual inspection conducted by an experienced researcher in the field of medical image analysis, we briefly evaluated the segmentation software by uploading the same CBCT DICOM files. Repeated segmentation of the same CBCT DICOM dataset from our study resulted in negligibly small deviation (GOM Inspect calculation of average mesh-to-mesh deviation was 0.08). We concluded that a consistency measurement was not necessary as the software we used had been extensively validated previously (Preda *et al.* 2022b). Based on the findings of our study, it can be concluded that utilizing AI-based segmentation, followed by LBF alignment with selection of the stable and adequately distributed RRAs, results in the most accurate registration of the sequential mandibular surface models.

Various methods and descriptors can be used to evaluate and visualise the registration accuracy. Color-coded deviation maps are widely used in digital dentistry as they provide a comprehensive representation of the extent and location of deviations (Nguyen *et al.* 2018; Ponce-Garcia *et al.* 2020; Revilla-León *et al.* 2021). In the present study, a discrete rather than a continuous scale was proposed to show the regions with deviations within a certain range of values for better understanding (Kuralt *et al.* 2020).

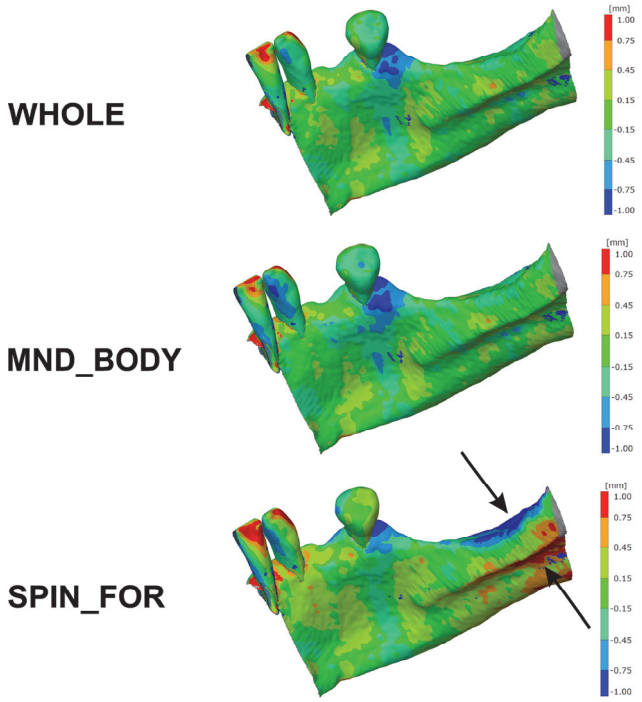


Fig. 5. *Visualization of the deviation between 3D mandibular model T0 and the model T1 when using different RRAs. The deviations are visualized with colour-coded deviation maps. The colour ranges are shown in a discrete scale for easier interpretation. Areas coloured red or dark blue (black arrowheads) represent the greatest deviation between the T0 and T1 models and indicate registration errors. The models are halved for better visualization.*

For quantitative measurements and statistical analyses, however, it is essential to supplement them with numerical descriptors. A commonly used measure is the root-mean-square error (RMSE) estimator (Koerich *et al.* 2016), which was originally intended as a metric to evaluate the performance of statistical models (Hodson 2022). Its suitability strongly depends on the distribution structure of the data (Hodson 2022). However, the calculation of the RMSE of the overall model does not include data on its distribution and does not quantify the rotational and translational shift of the models. To overcome this limitation, the distance between the T0 and T1 centroids of the mandibular canal outlines at each of the

three test sites (A, B and C) on the mandible was calculated. This approach assumes that the position of the mandibular canal in the adult mandible remains constant over time and that the segmentation of the canal is performed accurately. Using MND registration, the perfect overlap of the mandibular canal would indicate that the segmentation of the mandibular canal is reproducible. In this case, the median distance between the centroids of the mandibular canal would ideally be close to zero. In our study, it was measured at 0.09 mm. The midpoint of this distance served as the reference point at which the deviation of the other alignment methods was measured.

Based on the findings of the current study and relevant prior research, it is possible to offer general recommendations regarding the selection of the RRAs for surface-based registration. More important than the stability of the RRAs is its spatial distribution. It should be evenly distributed on 3D model (CBCT surface model, intraoral scan, facial scan) and should not form an imaginary axis. When the chosen RRA is small and positioned in the anterior region of the 3D model, minor inaccuracies in registration can have a magnified impact on the posterior portion (Stucki and Gkantidis 2020b; Kuralt and Fidler 2021).

The findings of the present study underscore the significance of bridging the knowledge gap between understanding the mathematic principles of best-fit algorithms and its clinical implications. Future study designs should aim to connect and integrate both these domains, allowing for a more comprehensive and impactful analysis. Our findings can drive future software developments or at least encourage a critical evaluation of the algorithms behind widely used, user-friendly applications. While many commercial software protocols are robust and easy to use, there is still room for improvement, as Garikano et al emphasise (Garikano *et al.* 2022). By prioritising accurate registration and rigorous selection of RRA, our approach has the potential to improve the accuracy of sequential evaluations over time and enable more reliable studies of bone resorption rates. In the field of oral and maxillofacial surgery, these results could be of great importance as precise registration methods allow for a thorough assessment of immediate surgical outcomes and support long-term evaluations of osteotomies, grafts and trauma reconstructions. Furthermore, these identical registration principles ought to be employed in 4D virtual patient applications, where the fusion of 3D entities from diverse data formats is required (Mangano *et al.* 2018; Joda *et al.* 2019).

Our study has some limitations. Firstly, a single CBCT device was used, possibly limiting the generalizability of the findings. Additionally, a single AI-assisted software was used for segmentation, introducing the potential for bias or variations specific to that software. Future studies should compare multiple CBCT devices and different automatic segmentation software. At present, exposure to radiation is prevalent with CBCT, and its use should be limited. Future development of post processing algorithms will enable imaging with substantially lower radiation doses (Friot-Giroux *et al.* 2022). Moreover, the use of non-invasive intraoral ultrasound with improved machine learning protocols for alveolar bone imaging is receiving great attention (Nguyen *et al.* 2020).

## CONCLUSION

The choice and spatial arrangement of RRAs critically affect the precision of aligning 3D models based on their surfaces. To enhance alignment accuracy, it's advisable to select RRAs on anatomically consistent areas that are widely spaced.

## ACKNOWLEDGMENTS

The work was supported by the Ministry of Higher Education, Science and Technology of the Republic of Slovenia, under grant number P3-0293.

## REFERENCES

Ahmad R, Abu-Hassan MI, Li Q, Swain M V (2013). Three dimensional quantification of mandibular bone remodeling using standard tessellation language registration based superimposition. Clin Oral Implants Res. 24(11):1273–79.

Besl PJ, McKay ND (1992). A method for registration of 3-D shapes. IEEE Trans Pattern Anal Mach Intell. 14(2):239–56.

Cui Z, Fang Y, Mei L, Zhang B, Yu B, Liu J, Jiang C, Sun Y, Ma L, Huang J, Liu Y, Zhao Y, Lian C, Ding Z, Zhu M, Shen D. (2022). A fully automatic AI system for tooth and alveolar bone segmentation from cone-beam CT images. Nat Commun. 13(1).

Friot-Giroux L, Peyrin F, Maxim V (2022). Iterative tomographic reconstruction with TV prior for low-dose CBCT dental imaging. Phys Med Biol. 67(20).

Garikano X, Amezua X, Iturrate M, Solaberrieta (2024). Evaluation of repeatability of different alignment methods to obtain digital interocclusal records: An in vitro study. J Prosthet Dent. 131(4):709–17.

Häner ST, Kanavakis G, Matthey F, Gkantidis N (2020). Voxel-based superimposition of serial craniofacial CBCTs: Reliability, reproducibility and segmentation effect on hard-tissue outcomes. Orthod Craniofac Res. 23(1):92–101.

Hodson TO (2022). Root-mean-square error (RMSE) or mean absolute error (MAE): when to use them or not. Geosci Model Dev. 15(14):5481–87.

Joda T, Gallucci GO, Wismeijer D, Zitzmann NU (2019). Augmented and virtual reality in dental medicine: A systematic review. Comput Biol Med. 108:93–100.

Koerich L, Burns D, Weissheimer A, Claus JDP (2016). Three-dimensional maxillary and mandibular regional superimposition using cone beam computed tomography: a validation study. Int J Oral Maxillofac Surg. 45(5):662–69.

Kondo T, Kanayama K, Egusa H, Nishimura I (2023). Current perspectives of residual ridge resorption: Pathological activation of oral barrier osteoclasts. J Prosthodont Res. 67(1):12–22.

Kuralt M, Fidler A (2021). Assessment of reference areas for superimposition of serial 3D models of patients with advanced periodontitis for volumetric soft tissue evaluation. J Clin Periodontol. 48(6):765–73.

Kuralt M, Gašperšič R, Fidler A (2020). 3D computer-aided treatment planning in periodontology: A novel approach for evaluation and visualization of soft tissue thickness. Journal of Esthetic and Restorative Dentistry. 32(5):457–62.

Kuralt M, Selmani Bukleta M, Kuhar M, Fidler A (2019). Bone and soft tissue changes associated with a removable partial denture. A novel method with a fusion of CBCT and optical 3D images. Comput Biol Med. 108:78–84.

Kuralt M, Selmani Bukleta M, Kuhar M, Fidler A (2022). A novel digital method for evaluation of mucosa thickness changes in time: changes associated with a removable partial denture. Image Anal Stereol. 41:181–91.

Lahoud P, Diels S, Niclaes L, Van Aelst S, Willems H, Van Gerven A, Quirynen M, Jacobs R (2022). Development and validation of a novel artificial intelligence driven tool for accurate mandibular canal segmentation on CBCT. J Dent. 116:103891.

Li P, Wang R, Wang Y, Tao W (2020). Evaluation of the ICP Algorithm in 3D Point Cloud Registration. IEEE Access. 8:68030–68048.

Liu X, Faes L, Kale AU, Wagner SK, Fu DJ, Bruynseels A, Mahendiran T, Moraes G, Shamdas M, Kern C, Ledsam JR, Schmid MK, Balaskas K, Topol EJ, Bachmann LM, Keane PA, Denniston AK (2019). A comparison of deep learning performance against health-care professionals in detecting diseases from medical imaging: a systematic review and meta-analysis. Lancet Digit Health. 1(6):e271–97.

Ma J, Schneider L, Lapuschkin S, Achtibat R, Duchrau M, Krois J, Schwendicke F, Samek W (2022). Towards Trustworthy AI in Dentistry. J Dent Res. 101(11):1263–68.

Mangano C, Luongo F, Migliario M, Mortellaro C, Mangano FG (2018). Combining intraoral scans, cone beam computed tomography and face scans: The virtual patient. J Craniofac Surg. 29(8):2241–46.

Mohammad-Rahimi H, Rokhshad R, Bencharit S, Krois J, Schwendicke F (2023). Deep learning: A primer for dentists and dental researchers. J Dent. 130:104430.

Nguyen KCT, Duong DQ, Almeida FT, Major PW, Kaipatur NR, Pham TT, Lou EHM, Noga M, Punithakumar K, Le LH (2020). Alveolar Bone Segmentation in Intraoral Ultrasonographs with Machine Learning. J Dent Res. 99(9):1054–61.

Nguyen T, Cevidanes L, Franchi L, Ruellas A, Jackson T (2018). Three-dimensional mandibular regional superimposition in growing patients. American Journal of Orthodontics and Dentofacial Orthopedics. 153(5):747–54.

De Oliveira Ruellas AC, Yatabe MS, Souki BQ, Benavides E, Nguyen T, Luiz RR, Franchi L, Cevidanes LHS (2016). 3D mandibular superimposition: Comparison of regions of reference for voxel-based registration. PLoS One. 11(6).

Oliveira-Santos N, Jacobs R, Picoli FF, Lahoud P, Niclaes L, Groppo FC (2023). Automated segmentation of the mandibular canal and its anterior loop by deep learning. Sci Rep. 13(1):10819.

O'Toole S, Osnes C, Bartlett D, Keeling A (2019). Investigation into the accuracy and measurement methods of sequential 3D dental scan alignment. Dental Materials. 35(3):495–500.

Ponce-Garcia C, Ruellas ACDO, Cevidanes LHS, Flores-Mir C, Carey JP, Lagravere-Vich M (2020). Measurement error and reliability of three available 3D superimposition methods in growing patients. Head Face Med. 16(1).

Preda F, Morgan N, Van Gerven A, Nogueira-Reis F, Smolders A, Wang X, Nomidis S, Shaheen E, Willems H, Jacobs R (2022a). Deep convolutional neural network-based automated segmentation of the maxillofacial complex from cone-beam computed tomography:A validation study. J Dent. 124.

Preda F, Morgan N, Van Gerven A, Nogueira-Reis F, Smolders A, Wang X, Nomidis S, Shaheen E, Willems H, Jacobs R (2022b). Deep convolutional neural network-based automated segmentation of the maxillofacial complex from cone-beam computed tomography:A validation study. J Dent. 124:104238.

Revilla-León M, Gohil A, Barmak AB, Zandinejad A, Raigrodski AJ, Alonso Pérez-Barquero J (2022). Best-Fit Algorithm Influences on Virtual Casts' Alignment Discrepancies. J Prosthodont: 32(4):331-339.

Revilla-León M, Pérez-Barquero JA, Barmak BA, Agustín-Panadero R, Fernández-Estevan L, Att W (2021). Facial scanning accuracy depending on the alignment

algorithm and digitized surface area location: An in vitro study. J Dent. 110.

Rischke R, Schneider L, Müller K, Samek W, Schwendicke F, Krois J (2022). Federated Learning in Dentistry: Chances and Challenges. J Dent Res. 101(11):1269–73.

Schneider L, Arsiwala-Scheppach L, Krois J, Meyer-Lueckel H, Bressem KK, Niehues SM, Schwendicke F (2022). Benchmarking Deep Learning Models for Tooth Structure Segmentation. J Dent Res. 101(11):1343–49.

Schwendicke F, Krois J (2022). Data Dentistry: How Data Are Changing Clinical Care and Research. J Dent Res. 101(1):21–29.

Schwendicke F, Samek W, Krois J. 2020. Artificial Intelligence in Dentistry: Chances and Challenges. J Dent Res. 99(7):769–74.

Schwendicke F, Singh T, Lee JH, Gaudin R, Chaurasia A, Wiegand T, Uribe S, Krois J (2021). Artificial intelligence in dental research: Checklist for authors, reviewers, readers. J Dent. 107.

Shaheen E, Leite A, Alqahtani KA, Smolders A, Van Gerven A, Willems H, Jacobs R (2021). A novel deep learning system for multi-class tooth segmentation and classification on cone beam computed tomography. A validation study: Deep learning for teeth segmentation and classification. J Dent. 115.

Song P (2015). Local voxelizer: A shape descriptor for surface registration. Comput Vis Media (Beijing). 1(4):279–89.

Spencer KR (2018). Implant based rehabilitation options for the atrophic edentulous jaw. Aust Dent J. 63:S100–07.

Stucki S, Gkantidis N (2020a). Assessment of techniques used for superimposition of maxillary and mandibular 3D surface models to evaluate tooth movement: A systematic review. Eur J Orthod. 42(5):559–70.

Stucki S, Gkantidis N (2020b). Assessment of techniques used for superimposition of maxillary and mandibular 3D surface models to evaluate tooth movement: A systematic review. Eur J Orthod. 42(5):559–70.

Tallgren A (1972). The continuing reduction of the residual alveolar ridges in complete denture wearers: A mixed-longitudinal study covering 25 years. J Prosthet Dent. 27(2):120–32.

Tan M, Cui Z, Zhong T, Fang Y, Zhang Y, Shen D (2024). A progressive framework for tooth and substructure segmentation from cone-beam CT images. Comput Biol Med. 169:107839.

Verhelst PJ, Smolders A, Beznik T, Meewis J, Vandemeulebroucke A, Shaheen E, Van Gerven A, Willems H, Politis C, Jacobs R (2021). Layered deep learning for automatic mandibular segmentation in cone-beam computed tomography. J Dent. 114.

Wang H, Minnema J, Batenburg KJ, Forouzanfar T, Hu FJ, Wu G (2021). Multiclass CBCT Image Segmentation for Orthodontics with Deep Learning. J Dent Res. 100(9):943–49.